# Identification of bone morphogenetic protein 7 (BMP7) as an instructive factor for human epidermal Langerhans cell differentiation

Nighat Yasmin,[1,3] Thomas Bauer,[1,3] Madhura Modak,[3] Karin Wagner,[2] Christopher Schuster,[4] Rene Köffel,[1,3] Maria Seyerl,[3] Johannes Stöckl,[3] Adelheid Elbe-Bürger,[4] Daniel Graf,[5] and Herbert Strobl[1,3]

[1]Institute of Pathophysiology and Immunology, Center for Molecular Medicine and [2]Center for Medical Research, Medical University Graz, A-8036 Graz, Austria
[3]Institute of Immunology, Center of Pathophysiology, Infectiology, and Immunology; and [4]Laboratory of Cellular and Molecular Immunobiology of the Skin, Department of Dermatology, Division of Immunology, Allergy, and Infectious Diseases; Medical University of Vienna, A-1090 Vienna, Austria
[5]Orofacial Development and Regeneration, Institute of Oral Biology, Center for Dental Medicine, University of Zurich, CH-8006 Zurich, Switzerland

**Human Langerhans cell (LC) precursors populate the epidermis early during prenatal development and thereafter undergo massive proliferation. The prototypic antiproliferative cytokine TGF-β1 is required for LC differentiation from human CD34+ hematopoietic progenitor cells and blood monocytes in vitro. Similarly, TGF-β1 deficiency results in LC loss in vivo. However, immunohistology studies revealed that human LC niches in early prenatal epidermis and adult basal (germinal) keratinocyte layers lack detectable TGF-β1. Here we demonstrated that these LC niches express high levels of bone morphogenetic protein 7 (BMP7) and that Bmp7-deficient mice exhibit substantially diminished LC numbers, with the remaining cells appearing less dendritic. BMP7 induces LC differentiation and proliferation by activating the BMP type-I receptor ALK3 in the absence of canonical TGF-β1–ALK5 signaling. Conversely, TGF-β1–induced in vitro LC differentiation is mediated via ALK3; however, co-induction of ALK5 diminished TGF-β1–driven LC generation. Therefore, selective ALK3 signaling by BMP7 promotes high LC yields. Within epidermis, BMP7 shows an inverse expression pattern relative to TGF-β1, the latter induced in suprabasal layers and up-regulated in outer layers. We observed that TGF-β1 inhibits microbial activation of BMP7-generated LCs. Therefore, TGF-β1 in suprabasal/outer epidermal layers might inhibit LC activation, resulting in LC network maintenance.**

CORRESPONDENCE
Herbert Strobl:
herbert.strobl@medunigraz.at

Abbreviations used: BMP, bone morphogenetic protein; EGA, estimated gestational age; FLT3L, fms-related tyrosine kinase 3 ligand; HPC, hematopoietic progenitor cell; IRES, internal ribosome entry site; LC, Langerhans cell; moDC, monocyte-derived DC; MPO, myeloperoxidase; PGN, peptidoglycan; SCF, stem cell factor; TARC, thymus and activation-regulated chemokine; TPO, thrombopoietin.

Langerhans cells (LCs) form dense cellular networks in basal/suprabasal layers of stratified epidermal and mucosal tissues. LCs are considered the environmentally exposed outposts of the immune system. They are capable of recognizing microbes and environmental substances and provide first-line innate antiviral immune defense. Moreover, they are capable of migrating to skin-draining lymph nodes and of inducing T cell–mediated adaptive immune responses to antigens encountered in the epidermis. This unique epidermal DC subset is developmentally dependent on the cytokine TGF-β1 as indicated by in vitro and in vivo data (Romani et al., 2012; Igyártó and Kaplan, 2013).

TGF-β1 was identified as a factor inducing LC differentiation from human monocytopoietic cells in vitro (Strobl et al., 1996). Although in the absence of TGF-β1 cytokine-stimulated CD34+ hematopoietic progenitor cells (HPCs) developed into monocyte/macrophages, supplementation of these cultures with TGF-β1 directed progenitor cell differentiation toward LCs (Strobl et al., 1996, 1997). In line with this, neutralizing anti–TGF-β1 antibody abrogated LC differentiation (Caux et al., 1999), demonstrating that endogenous TGF-β1 in these cultures (Caux et al., 1992) is required for the induction of LC differentiation. Congruent with these observations,



The Rockefeller University Press $30.00
J. Exp. Med. 2013 Vol. 210 No. 12 2597-2610
www.jem.org/cgi/doi/10.1084/jem.20130275



The Journal of Experimental Medicine

blood monocytes acquire LC characteristics in response to TGF-β1 stimulation (Geissmann et al., 1998; Hoshino et al., 2005). Mouse in vivo data similarly demonstrated that LC differentiation depends on TGF-β1. LC networks are absent from TGF-$\beta1^{-/-}$ mice (Borkowski et al., 1996), and the specific deletion of TGF-β1 and TGF-βRII in LCs resulted in reduced numbers of epidermal LCs, indicating that TGF-β1 acts directly on LC differentiation (Kaplan et al., 2007). Congruent with these observations, LC networks were impaired in mice deficient for TGF-β1 downstream signaling molecules Id2 (Hacker et al., 2003) and Runx3 (Fainaru et al., 2004). Together, these observations firmly established a key role of TGF-β1 during LC differentiation.

However, recent data challenged the view that TGF-β1 is required for LC differentiation. First, LCs possess substantial proliferative capacity in the steady-state (Merad et al., 2002), as well as during prenatal life or during inflammation (Chang-Rodriguez et al., 2005; Chorro et al., 2009; Schuster et al., 2009). These findings seem to be incompatible with the well-defined antiproliferative function of TGF-β1 (Dennler et al., 2002). Second, basal keratinocyte layers are devoid of TGF-β1 expression, which has been considered critical for keratinocyte stem cell proliferation (Li et al., 2006). Some LCs reside in basal keratinocyte layers, and Ki67 staining revealed that a fraction of these cells undergo proliferation in the steady-state adult skin (Schuster et al., 2009). Third, LC precursor seeding of the prenatal epidermis precedes TGF-β1 expression induction in the epidermis (Schuster et al., 2009). Fourth, the deletion of components of the canonical TGF-β1 signaling cascade still allowed normal LC differentiation in vivo. Canonical TGF-β1 signaling is transmitted via the type-I receptor ALK5 and also depends on type-II receptors, leading to the downstream activation of transcription factors Smad2/3 (Massagué, 1998). Deficiency of Smad3 failed to impair LC networks (Xu et al., 2012). Similarly, the deletion of ALK5 from $CD11c^+$ or $CD207^+$ cells allowed LC differentiation, as revealed by the presence of LC networks at birth; only postnatally did LC numbers rapidly drop as a result of the emigration of LCs from the epidermis to lymph nodes shortly after birth (Kel et al., 2010; Zahner et al., 2011). Consistently, the conditional deletion of TGF-β1 and TGF-βRII in LCs resulted in their migration to the lymph nodes, likely because of enhanced proinflammatory cytokine production and LC activation (Bobr et al., 2012). TGF-β1 also interferes with the maturation and proinflammatory cytokine production by monocyte-derived DCs (moDCs; Geissmann et al., 1999). Collectively, canonical TGF-β1–ALK5–Smad3 signaling seems to be critical for postnatal LC network maintenance but does not seem to be required for LC differentiation.

Although ALK5 is regarded as the classical TGF-β1 receptor, TGF-β1 can also activate other type-I receptors such as ALK1 (Oh et al., 2000; Goumans et al., 2002), ALK2, and ALK3 (Ebner et al., 1993; Daly et al., 2008). ALK receptors form hetero- and homooligomers that are differentially activated by members of the TGF-β/bone morphogenetic protein (BMP) superfamily (Miyazono et al., 2010). Considering the aforementioned recent observations that TGF-β1 might not be critical for LC differentiation, we considered deciphering the mechanism underlying LC differentiation to be of major importance. Here we identified BMP7 as a key factor inducing LC differentiation.

## RESULTS

### TGF-β1 promotes LC differentiation through the type-I receptor ALK3

TGF-β1 is the classical ligand for ALK5, whereas ALK2 and ALK3 receptors are activated by both TGF-β1 (Daly et al., 2008) and BMP (Miyazono et al., 2010). We aimed to explore the downstream signaling mechanism governing TGF-β1–dependent LC differentiation. Hence, we added or did not add inhibitors of ALK4/5/7 (SB421543) or ALK2/3/6 (dorsomorphin) to LC generation cultures. $CD34^+$ cells were pretreated for 1 h with either compound and were subsequently induced to differentiate into LCs in the presence of GM-CSF, stem cell factor (SCF), TNF, fms-related tyrosine kinase 3 ligand (FLT3L), and TGF-β1. Without inhibitors, a fraction of day 3–generated cells readily exhibited LC phenotypic characteristics ($CD1a^+CD207^+$). Unexpectedly, ALK5 inhibition led to the generation of increased percentages of LCs, indicating that the canonical TGF-β1/ALK5 downstream signaling is not only dispensable for LC generation but even negatively affects it (Fig. 1 A, left). In sharp contrast, interference with ALK2/3/6 receptor signaling strongly impaired LC generation, as indicated by a substantial drop in percentages of LCs (Fig. 1 A, right). Consistently, the total numbers of day 7–generated LCs were higher in the presence of the ALK5 inhibitor in all three experiments analyzed (Fig. 1 B). In comparison, day 7 cultures in the presence of ALK2/3 inhibitor did not contain any viable cells (not depicted), indicating that ALK2/3 signaling rather than ALK5 is critical for TGF-β1–dependent LC differentiation from progenitor cells.

To confirm these data, we transduced $CD34^+$ cells with retroviral vectors encoding ALK2–, ALK3–, or ALK5–internal ribosome entry site [IRES]–GFP or empty control vector. Subsequently, we generated LCs from $CD34^+$ cells as previously reported (Strobl et al., 1997). $GFP^+$ gated cells were analyzed for LC characteristics. ALK3-transduced cells contained significantly higher percentages of $CD207^+CD1a^+$ cells as compared with empty control vector–transduced cells. Moreover, neither ectopic ALK2 nor ALK5 resulted in altered percentages of LCs (Fig. 1 C). Together with the observation that ALK3 is expressed in the epidermis (Botchkarev et al., 1999; Hwang et al., 2001), our loss and gain of function experiments indicate that TGF-β1 utilizes ALK3 signaling for promoting LC differentiation.

LC generation cultures contained only very low percentages of cells expressing CD11b and/or CD14, which did not change significantly in response to addition of ALK inhibitors (Fig. 1 A). Moreover, ectopic ALK3 expression failed to promote the generation of cells expressing CD14, CD11b or the early myeloid marker myeloperoxidase (MPO) in LC generation cultures (Fig. 1 D). Similarly, ectopic ALK3 neither modulated

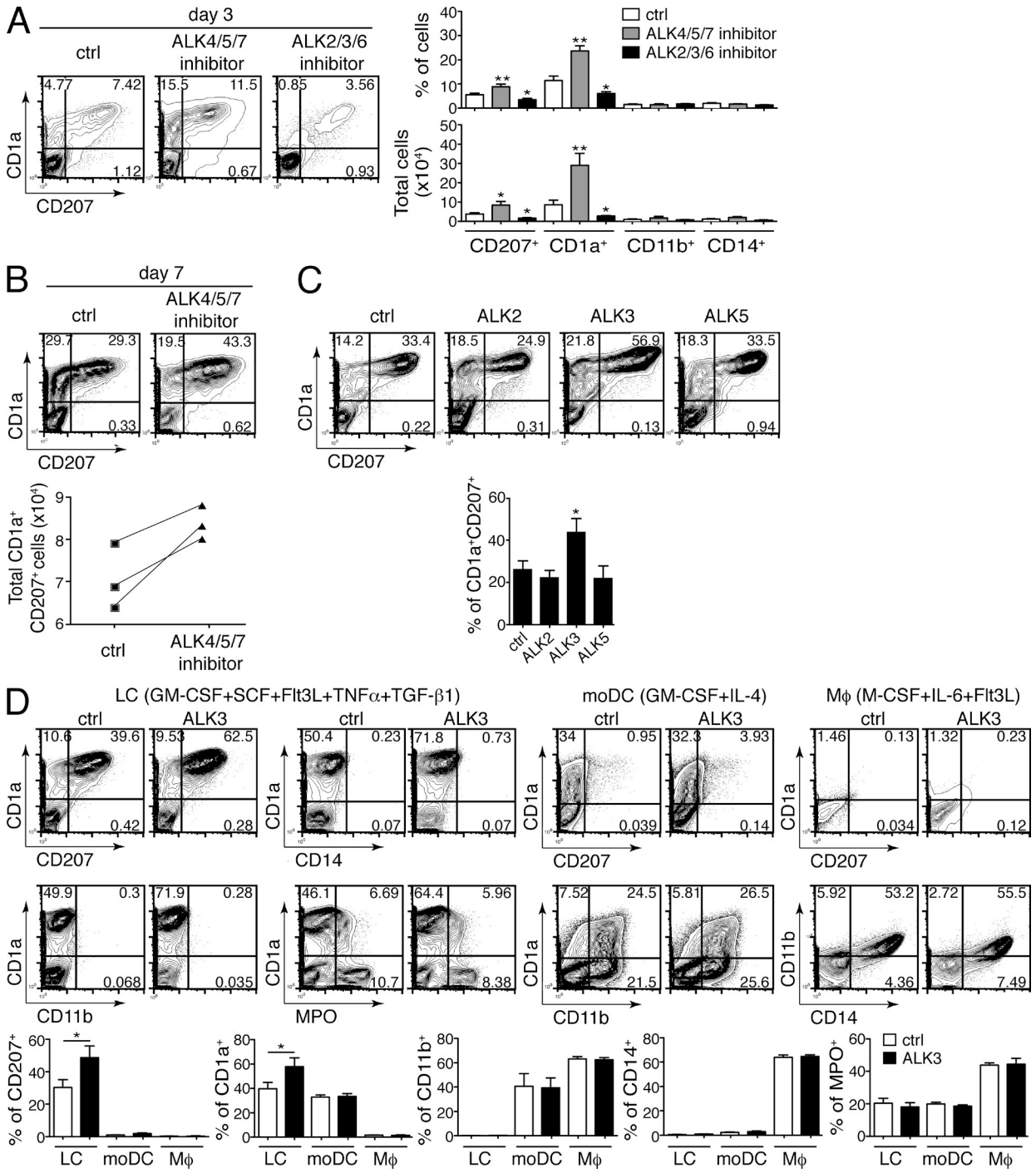


**Figure 1. TGF-β1 induces LC differentiation through type-I receptor ALK3.** (A) Pre-expanded CD34⁺ cells were treated or not with ALK4/5/7 inhibitor (SB421543) or ALK2/3/6 inhibitor (dorsomorphin) for 1 h before TGF-β1 addition. FACS plots represent day 3–generated LCs in the presence or absence of inhibitors analyzed for CD1a⁺CD207⁺ by flow cytometry. Data are representative of six independent experiments. Bar diagrams represent percentages and total numbers of cells expressing CD1a⁺CD207⁺, CD1a⁺, CD11b⁺, or CD14⁺ cells (±SEM; *, $P < 0.05$; **, $P < 0.004$). (B) Day 7–generated LCs were incubated in the presence or absence of SB421543 and analyzed for CD1a and CD207 by flow cytometry. Data are representative of three independent experiments. Graph represents total numbers of CD1a⁺CD207⁺ cells. (C) CD34⁺ cells were transduced with retroviral vectors encoding ALK2-, ALK3-, or ALK5-IRES-GFP and were cultured in the presence of TGF-β1. FACS plots represent day 7–generated GFP⁺ cells analyzed for CD1a and CD207. Data are representative of three independent experiments. Bar diagram represent percentages of CD1a⁺CD207⁺ cells (±SEM; *, $P < 0.05$). (D) CD34⁺ cells were transduced with retroviral vector encoding ALK3-IRES-GFP and cultured in LC, moDC, and monocyte/macrophage (Mϕ) lineage conditions. FACS plots represent day 7–generated GFP⁺ cells analyzed for CD1a, CD207, CD11b, CD14, and MPO. Bar diagrams represent percentages of CD1a⁺, CD207⁺, CD11b⁺, CD14⁺, and MPO⁺ cells. Data are representative of four independent experiments (±SEM; *, $P < 0.05$).

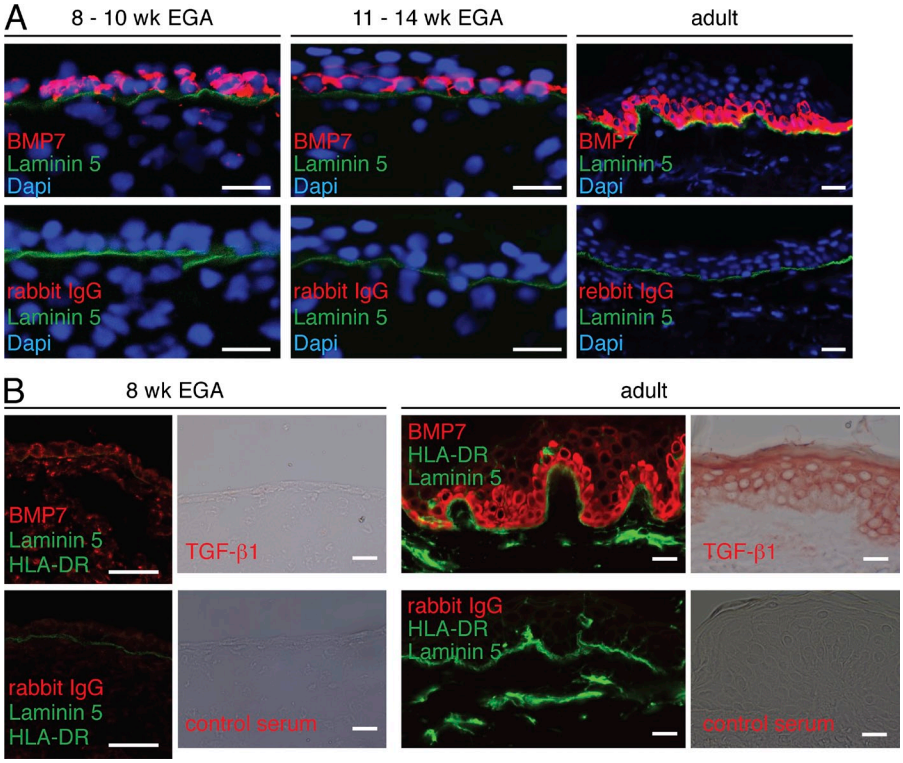


**Figure 2. BMP7 expression is detectable in the basal epidermis during human prenatal development.** (A) 6-µm skin sections from prenatal and adult human skin were analyzed for the expression of BMP7 or control. Nuclei and the dermo-epidermal junction were visualized with DAPI and mAb directed against Laminin 5, respectively. Data are representative of three donors for 8–10 wk EGA, two donors for 11–14 wk EGA, and three donors for healthy adult skin. (B) Immunofluorescence staining of BMP7 and HLA-DR at 8 wk EGA and adult human skin. Immunohistochemical staining was performed on cryostat sections. TGF-β1 was visualized with AEC. Data are representative of two independent experiments. Bars, 50 µm.

percentages of cells exhibiting a $CD11b^+CD1a^+CD207^-$ moDC phenotype nor a $CD14^+CD11b^+$ monocyte/macrophage phenotype generated in specific cytokine combinations (Fig. 1 D). Therefore, ALK3 specifically promoted the generation of $CD1a^+$ $CD207^+$ LCs among the various cell subsets analyzed.

### BMP7 is detectable in the basal epidermal layer during human prenatal development

Among various ALK3 ligands, only BMP7 has a predominant expression pattern in basal keratinocyte layers (Takahashi and Ikeda, 1996). Moreover, only BMP7 is strongly expressed in fetal epidermis at day 17.5 postcoitum. (Helder et al., 1995), a time window when LC precursors first appear in the fetal mouse epidermis (Romani et al., 1986; Elbe et al., 1989; Chang-Rodriguez et al., 2005; Chorro et al., 2009). However, human data on the distribution of BMP7 among keratinocyte layers during prenatal development were lacking. We previously identified proliferating LCs in basal layers of human epidermis (Schuster et al., 2009) and demonstrate here that BMP7 is detectable in the epidermis from the earliest time point analyzed (8–10 wk estimated gestational age [EGA]; Fig. 2 A). Stratified epidermis at subsequent time points (11–14 wk EGA, adult) contains BMP7 exclusively in basal/suprabasal layers (Fig. 2 A). In comparison, TGF-β1 cannot be detected in the epidermis at 8 wk EGA (Fig. 2 B; Schuster et al., 2009). Moreover TGF-β1 is undetectable in the basal epidermal layer and is only found suprabasally (Fig. 2 B; Kane et al., 1990; Schuster et al., 2009). Therefore, we conclude that BMP7 expression precedes TGF-β1 expression during embryonic epidermal development, and both molecules show an inverse expression pattern in the stratified epidermis: TGF-β1 exclusively suprabasally and BMP7 in the basal/germinative layer (Fig. 2 B). Given that epidermal LC precursors can be detected at 8–11 wk EGA (Schuster et al., 2009) and reside in basal/suprabasal keratinocyte layers, these cells are primarily exposed to a $BMP7^+$ $TGF\text{-}\beta1^-$ microenvironment. Only LCs in suprabasal epidermal layers are also exposed to TGF-β1.

### Numeric and morphological LC impairment in Bmp7-deficient mice

To study the potential role of BMP7 during LC differentiation in vivo, we analyzed Bmp7-deficient mice (Zouvelou et al., 2009). These mice die shortly after birth, limiting the analysis of the LC differentiation process. However, IA/IE-positive LCs can be already detected right after birth (postnatal day [P] 0; Chorro et al., 2009). To assess the expression pattern of BMP7, epidermal sheets from Bmp7-LacZ mice were stained with X-gal. Widespread expression of BMP7 in mouse keratinocytes was detected (Fig. 3 A), similar to human epidermal sections as shown in Fig. 2. Epidermal LC precursor cells acquire MHCII around birth (P0), with detectable langerin/CD207 expression appearing at P2 (Chorro et al., 2009). We therefore analyzed mice at P0 using antibodies against IA/IE (MHCII). Bmp7-deficient mice (P0) showed substantial reductions in epidermal $MHCII^+$ cell frequencies (Fig. 3 B). Interestingly, the $MHCII^+$ cells in these mice exhibited lower numbers of dendritic processes compared with cells from WT littermate controls (Fig. 3 C).

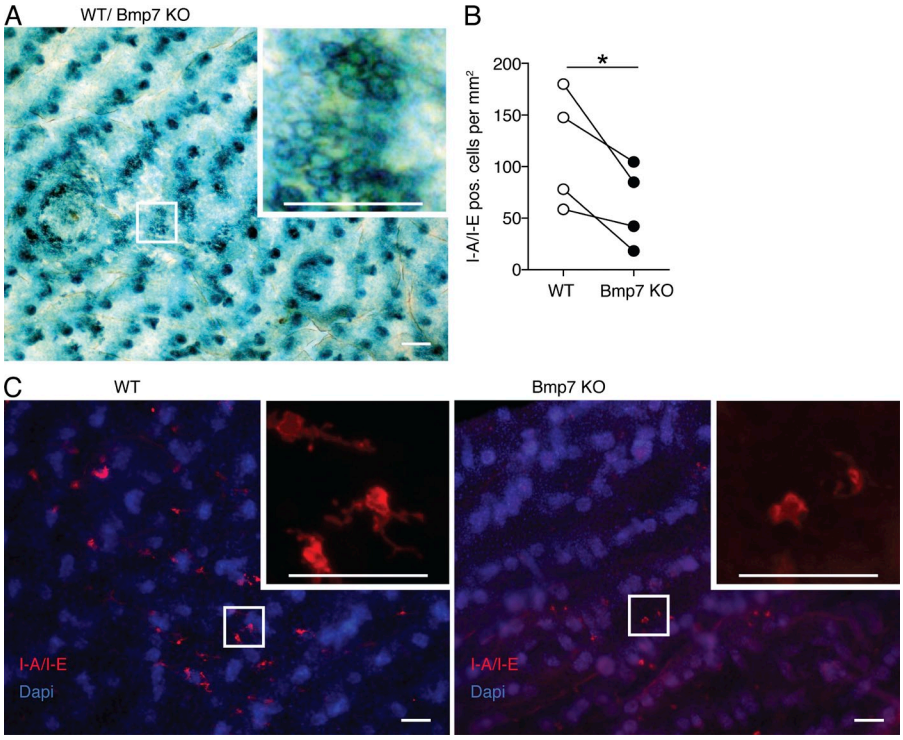


**Figure 3. LC impairment in Bmp7-deficient mice.** (A) Tissues from heterozygous *Bmp7lacZ* (*Bmp7*$^{wt/lacZ}$) mice (expressing β-galactosidase under the control of the *Bmp7* promoter) were stained with X-gal to identify the location of *Bmp7* expression. The transcriptional activity of Bmp7 is revealed by lacZ staining in the epidermis of BMP7-lacZ mice. One representative image from three different mice and experiments is shown. (B) I-A/I-E–positive cells from the epidermis of WT and Bmp7 KO mice at birth (P0) were enumerated and shown in I-A/I-E$^+$ cells/mm$^2$. Graph shows the number of I-A/I-E$^+$ cells, with each connected open and closed dot representing mean data from one independent litter. *, $P < 0.05$. (C) Representative immunofluorescence staining of an epidermal sheet from a WT and a BMP7 KO mouse. LCs were visualized with antibodies against I-A/I-E, and nuclei were stained with DAPI. Data are representative of four independent experiments. Insets represent higher magnification of the framed areas. Bars, 50 µm.

### BMP7-dependent activation of ALK3-Smad1/5/8 promotes LC differentiation

Considering the aforementioned in vitro and in vivo observations, we hypothesized that BMP7 might act as TGF-β1–independent positive regulator of LC differentiation and that the selective triggering of ALK3 by BMP7 might enable amplified LC generation. Thus, we added BMP7 instead of TGF-β1 to LC generation cultures and monitored percentages and total numbers of LCs. A hallmark characteristic of TGF-β1–induced in vitro generated LCs is the formation of huge macroscopically visible homotypic E-cadherin–mediated LC clusters (Fig. 4 A). Strikingly, BMP7 alone induces higher frequencies of LC clusters as well as on average higher percentages of E-cad$^+$CD1a$^+$CD207$^+$ cells than TGF-β1 when added to these cultures (Fig. 4 A). Accordingly, total numbers of CD1a$^+$ E-cad$^+$CD207$^+$ cells were significantly higher in BMP7 than in TGF-β1–supplemented cultures (Fig. 4 A). Therefore, BMP7 by far exceeds TGF-β1 in promoting LC generation. These observations are congruent with the aforementioned positive role of ALK3 in LC differentiation and with the observations that ALK5 (induced by TGF-β1 but not BMP7) inhibits LC generation. CFSE-labeling experiments confirmed superior proliferation of cells from BMP7-supplemented cultures relative to TGF-β1–treated cells (Fig. 4, B and C).

In subsequent experiments we performed a side-by-side comparison of BMP7 with other BMPs known to be expressed in the adult epidermis (i.e., BMP2, BMP4, and BMP6 [Botchkarev, 2003]). Dose response experiments revealed that only BMP4 replaced BMP7 in inducing LC differentiation. Conversely, neither BMP2 nor BMP6 induced LC generation (not depicted). Immunohistology revealed that BMP4 is not detectable in human prenatal epidermis (not depicted), consistent with the fact that BMP4 expression cannot be detected in interfollicular epidermis (Lyons et al., 1989; Bitgood and McMahon, 1995).

In subsequent experiments, we treated LC precursors with either TGF-β1 or BMP7 and analyzed the phosphorylation of Smad proteins. TGF-β1 induces phosphorylation of Smad2/3 (a signature of TGF-β signaling via ALK5) and Smad1/5/8 (a signature of canonical BMP signaling via ALK2/3; Feng and Derynck, 2005; Schmierer and Hill, 2007). Conversely, BMP7 resulted in Smad1/5/8 phosphorylation only (Fig. 5 A; Izumi et al., 2006). We next determined the expression levels of ALK2, ALK3, and ALK5 receptors in TGF-β1 LCs or BMP7 LCs by qRT-PCR analysis during LC differentiation. TGF-β1–generated LCs exhibit higher expression levels of ALK5 than ALK3. Conversely, an inverse expression pattern was observed for BMP7-generated LCs (ALK3 > ALK5; Fig. 5 B). TGF-β1 is known to be auto-induced by canonical TGF-β1–ALK5 signaling. Accordingly, TGF-β1 mRNA was induced in TGF-β1–supplemented LC generation cultures. Conversely, BMP7-supplemented LC generation cultures did not exhibit induction of TGF-β1 mRNA (Fig. 5 C). These observations are consistent with our finding that LC differentiation occurs independently of ALK5/Smad2/3 signaling.

### BMP7-generated LCs produce higher amounts of proinflammatory cytokines in response to microbial signals than TGF-β1–generated LCs

TGF-β1 inhibits proinflammatory cytokine production and DC maturation (Geissmann et al., 1999). Accordingly, ALK5 deficiency in LCs resulted in their spontaneous egress from

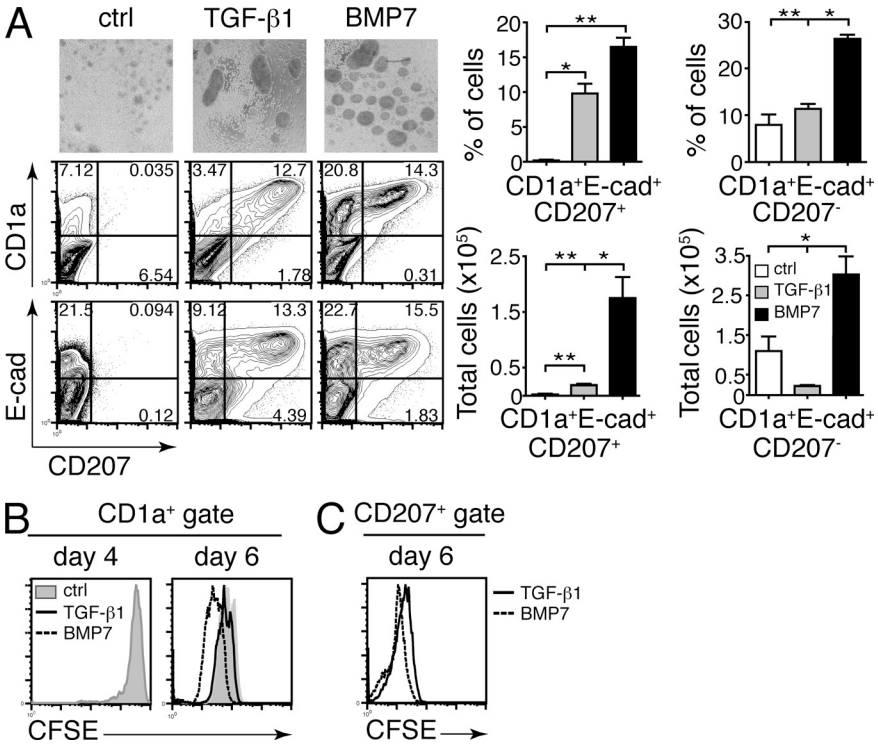


**Figure 4. BMP7 induces LC differentiation.** (A) CD34+ cells were incubated with GM-CSF, FLT3L, SCF, and TNF in the presence of TGF-β1, BMP7, or control, and morphology was assessed. FACS plots represent day 7–generated cells analyzed for the expression of CD1a, CD207, and E-cadherin. Bar diagrams represent percentages and total numbers of phenotypically defined cells generated as indicated. Data are representative of three independent experiments (mean ± SEM; *, $P < 0.05$; **, $P < 0.005$). (B and C) Cells were labeled with CFSE at day 4. CD1a+ cells (left; data are representative of four independent experiments) and CD207+ cells (right; data are representative of three independent experiments) were analyzed at day 6 by flow cytometry.

the postnatal epidermis, and this effect was accompanied by LC activation/maturation (Kel et al., 2010). We analyzed whether BMP7-ALK3–dependent LCs show enhanced cytokine production relative to TGF-β1–induced LCs. LCs generated in the presence of BMP7 or TGF-β1 form large clusters allowing enrichment of E-cad+CD1a+CD207+ LCs using 1g-sedimentation (Fig. 6 A; Gatti et al., 2000). LCs generated under both conditions showed similar up-regulation of T cell co-stimulatory molecules CD86 and CD83 in response to TLR ligands peptidoglycan (PGN) and Pam3CSK4 (Fig. 6 B). However, PGN-treated BMP7 LCs produced substantially higher amounts of proinflammatory cytokines (TNF, IL-1β, IL-6, IL-12p40, and IL-12p70) along with higher levels of immunosuppressive cytokine IL-10 compared with TGF-β1 LCs (Fig. 6 C). In the absence of TLR ligand, BMP7- or TGF-β1–generated LCs exhibited similar low expression levels of proinflammatory cytokines (Fig. 6 C).

Moreover, TLR-stimulated BMP7-generated LCs possessed higher allogeneic T cell immunostimulatory capacity than TGF-β1–generated LCs in 12 out of 14 independent experiments (Fig. 6 D). Additionally, these two LC populations differed in the induction of T helper (Th) responses from adult allogeneic T cells. Specifically, TGF-β1 LCs expressed high levels of the Th2-type chemokine thymus and activation-regulated chemokine (TARC)/CCL17 than BMP7 LCs. Consistently, TGF-β1 LCs induced T cells producing higher amounts of IL-13 and IL-5 (affiliated with Th2 responses); vice versa, BMP7 LCs induced higher amounts of IFN-γ (affiliated with Th1 responses; Fig. 6, E and F). Lower cytokine production from cord blood T cells as compared with adult peripheral blood T cells (Fig. 6 F) is in line with previous observations (Gupta et al., 2005).

### Genome-wide analysis shows similar gene expression by TGF-β1 and BMP7 LCs

To rule out the possibility that the aforementioned differences in cytokine production and T cell stimulation of TGF-β1 LCs versus BMP7 LCs are caused by differences in cell lineage identity, we performed genome-wide cDNA microarray analyses of flow-sorted CD1a+CD207+ cells. Both populations clustered together in terms of gene expression pattern observed in three independent experiments (Fig. 7, donors A, B, and C). Moreover, comparison with recently deposited datasets (Hutter et al., 2012; Lundberg et al., 2013) revealed a closer resemblance to ex vivo isolated human LCs (Hutter et al., 2012) than to CD34+ cell–derived LCs described in a recent study (Lundberg et al., 2013). This latter study used a different cytokine combination to generate LCs (i.e., IL-4 instead of FLT3L), potentially explaining the observed differences. For example, it was previously reported that IL-4 antagonizes the induction of certain TGF-β1–induced LC marker characteristics when added to cultures of CD34+ progenitor cells containing GM-CSF and TNF (Caux et al., 1999).

### Late addition of TGF-β1 to BMP7-supplemented cultures enhances percentages of CD207+CD1a+ LCs

Whereas percentages of CD207+CD1a+ cells generated in the presence of TGF-β1 or BMP7 were equivalent, total cellularity was much higher in BMP7- than in TGF-β1–supplemented cultures (Fig. 4 A). We observed that BMP7-supplemented cultures contain markedly higher percentages of CD1a+E-cad+ cells that lacked CD207 (Fig. 4 A). Large percentages of these cells positively correlated with larger LC cluster numbers present in these cultures, indicating that these

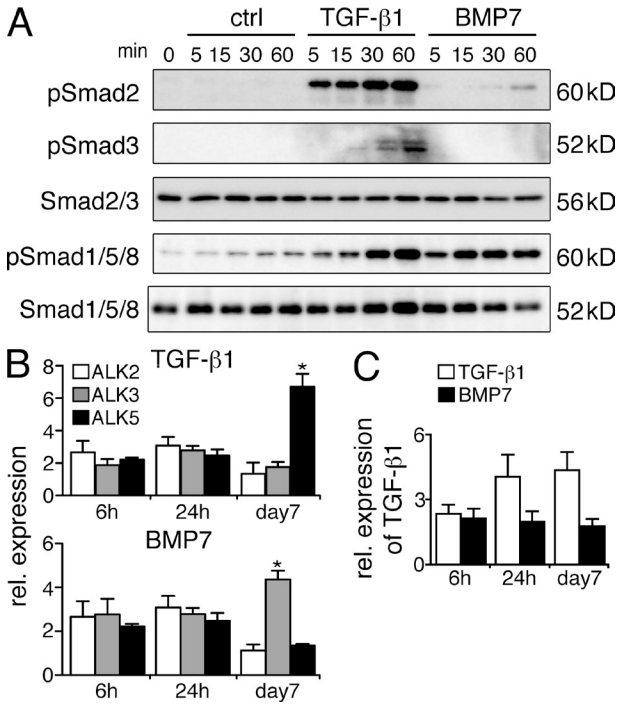


**Figure 5. Activation of Smad1/5/8 drives LC differentiation.** (A) Pre-expanded CD34+ cells were treated with TGF-β1 or BMP7 for the indicated times. Levels of immunoblot pSmad2/3, Smad2/3, pSmad1/5/8, and Smad1/5/8 were analyzed. Data are representative of five independent experiments. (B) LCs were generated in the presence of TGF-β1 or BMP7, and expression of ALK2, ALK3, and ALK5 was assessed during LC differentiation by qRT-PCR. Values were normalized to HPRT. Data are representative of three independent experiments (±SD; *, $P < 0.05$). (C) TGF-β1 expression during LC differentiation was assessed by qRT-PCR. Data are representative of three independent experiments (±SD).

cells may represent immediate precursors of LCs still capable of proliferation. Thus, we hypothesized that TGF-β1 might inhibit cell cycle progression, in turn allowing terminal LC differentiation, similarly as previously observed for erythropoiesis (Krystal et al., 1994). Hence, we analyzed whether $CD1a^+E\text{-}cad^+CD207^-$ cells from BMP7 LC–generated cultures can be induced to differentiate into $CD1a^+E\text{-}cad^+CD207^+$ cells by the late addition of TGF-β1. Adding TGF-β1 to BMP7 LC–generated cultures at day 5 indeed resulted in higher percentages of $CD1a^+E\text{-}cad^+CD207^+$ cells within 48 h, and this effect was accompanied by diminished percentages of $CD1a^+E\text{-}cad^+CD207^-$ cells. Using this two-step culture system (BMP7, 5 d, followed by TGF-β1 for 48 h), very high numbers of $CD1a^+E\text{-}cad^+CD207^+$ LCs were generated (Fig. 8 A). The first culture phase (BMP7 supplemented, no TGF-β1) can be prolonged from 5 to 7 d (not depicted). Conversely, when TGF-β1 was added at day 0 to BMP7-supplemented cultures, similar cellularity and percentages of LCs were observed as for TGF-β1 alone (not depicted). Therefore, TGF-β1 effects dominate over BMP7 effects on cell proliferation in LC generation cultures.

### BMP7 strongly promotes LC generation in serum-free medium devoid of TNF and SCF

Given the strong effect of BMP7 on LC generation, we asked in subsequent experiments whether BMP7 signaling might allow elimination of other cytokine stimuli present in this culture model. Therefore, the aforementioned two-step protocol was used for cytokine omission experiments. Specifically, we analyzed consequences of omission of individual or combinations of cytokines from the first culture phase. The omission of FLT3L led to substantially decreased percentages and numbers of LCs. Conversely, omission of both TNF and SCF, two factors which were previously shown to be critical for LC generation (Caux et al., 1992; Young et al., 1995), did not affect LC generation (Fig. 8 B). Therefore, a cytokine combination containing BMP7, GM-CSF, and FLT3L followed by TGF-β1 for the final 48 h efficiently induces the generation of $CD207^+$ $CD1a^+$ LCs from progenitor cells. In conclusion, the addition of BMP7 allows the elimination of two critical cytokines from previously optimized LC generation protocols.

### TGF-β1 inhibits proinflammatory cytokine production by BMP7-generated LCs

Although TGF-β1–generated LCs produce much lower levels of proinflammatory cytokines than BMP7-generated LCs in response to microbial stimuli (Fig. 6 C), LCs generated by using the sequential protocol (6 d BMP7, followed by 48 h TGF-β1) equaled LCs from TGF-β1–supplemented LC generation cultures (Fig. 8 C). Therefore, TGF-β1 strongly impairs proinflammatory cytokine production from BMP7-generated LCs.

## DISCUSSION

LCs reside within basal and suprabasal epidermal layers in adult human skin. During prenatal development, already the single-layered epidermis is populated by LC precursors and undergoes considerable proliferation to allow a tight LC network formation before birth. Also in adult epidermal basal layers, a small portion of LCs proliferates as indicated by the expression of Ki67 (Schuster et al., 2009). We here showed that LCs entering the epidermis are initially exposed to a $BMP\text{-}7^{hi}$ environment. BMP7 is strongly expressed in embryonic epidermis at 8 wk EGA, a time point when LC precursors are first detectable in human embryonic skin. In stratified epidermis in fetal and adult skin, BMP7 expression is restricted to basal and suprabasal keratinocyte layers but is lost in outer epidermal layers. Inversely, TGF-β1 is induced in suprabasal layers only and is up-regulated in outer epidermal layers (Kane et al., 1990; Schuster et al., 2009). Therefore, TGF-β1 shows a reciprocal distribution versus BMP7 in the epidermis. Consistently, BMP7 expression (EGA week 8) precedes TGF-β1 induction (EGA week 11, restricted to outer keratinocyte layers) during fetal epidermal development.

We further demonstrated that BMP7 induces LC differentiation accompanied by massive cell proliferation in vitro. Conversely, TGF-β1 inhibited LC activation and proliferation dominantly when added to BMP7-dependent LC generation cultures. BMP7 activates ALK3 (canonical BMP signaling) in

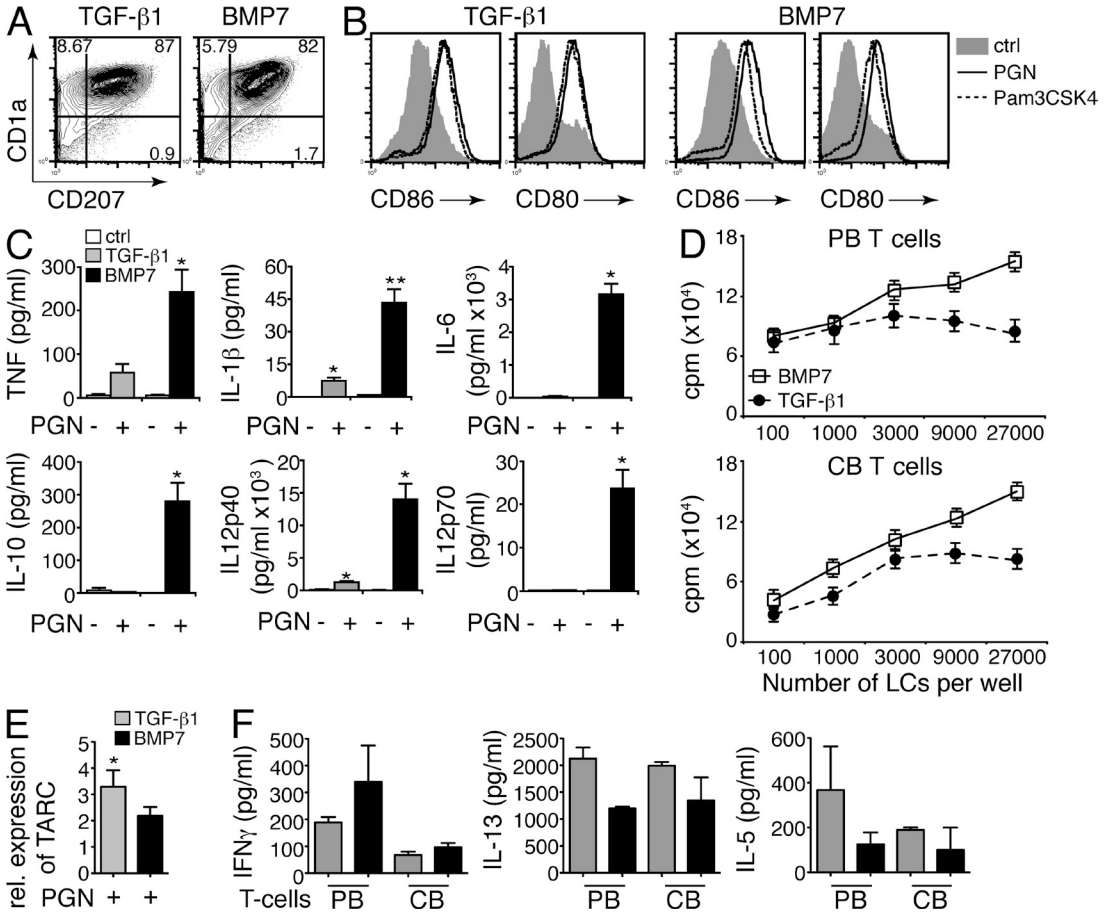


**Figure 6. Higher proinflammatory cytokine production by BMP7-generated microbial-stimulated LCs.** (A) Expanded CD34⁺ cells were induced to differentiate into LCs in response to TGF-β1 or BMP7 stimulation as in Fig. 4 A. LC clusters were purified using 1g sedimentation, and CD1a and CD207 expression was analyzed by flow cytometry. Data are representative of four independent experiments. (B) Cluster-purified LCs (TGF-β1 or BMP7) were activated or not with PGN or Pam3CSK4 for 2 d, and CD80 and CD86 expression was analyzed by flow cytometry. Data are representative of four independent experiments. (C) Cluster-purified LCs (TGF-β1 or BMP7) were activated or not with PGN for 2 d, and supernatants were collected for cytokine measurement. Bar diagrams represent amounts of cytokines produced. Data are representative of four independent experiments (±SD; *, $P < 0.05$; **, $P < 0.005$). (D) $10^5$ T cells were stimulated with the indicated numbers of LCs. Proliferation of T cells was monitored on day 5 of culture by adding [methyl-$^3$H]TdR, followed by measuring [methyl-$^3$H]TdR incorporation 18 h later. Error bars represent SEM of triplicate values. Data are representative of 14 independent experiments (CB, cord blood; PB, peripheral blood). (E) TGF-β1– or BMP7-generated LCs were stimulated with PGN for 2 d, and TARC expression was analyzed by qRT-PCR. Data are representative of four independent experiments (±SEM; *, $P < 0.05$). (F) Allogeneic T cells were co-cultured with activated TGF-β1 or BMP7 LCs, and production of IFN-γ, IL-13, and IL-5 was measured by using the Luminex system. Data are representative of four independent experiments (±SEM).

the absence of ALK5 (canonical TGF-β1 signaling). On the contrary, TGF-β1 activates both cascades. We showed by gain and loss of function experiments that ALK3 signaling promotes LC differentiation. Together, presented data in this study indicate that LC differentiation and proliferation are induced by BMP7-ALK3 in the absence of canonical TGF-β1–ALK5 signaling. Instead, canonical TGF-β1–ALK5 signaling has an important role for the maintenance of LC networks after birth (Kel et al., 2010). We showed that the addition of TGF-β1 to BMP7-generated LCs inhibits TLR-mediated LC activation. Because the epidermis is populated with commensal bacteria immediately after birth, TGF-β1 in suprabasal/outer epidermal layers might inhibit LC activation, which in turn may secure LC network maintenance.

TGF-β1 inhibits LC activation at least in part by inducing negative signaling proteins such as Axl (Bauer et al., 2012), which contribute to low proinflammatory cytokine production in LCs. In support for this model, in vitro BMP7-generated LCs lacked Axl (unpublished data). Moreover, basal keratinocyte layers and LCs located in basal layers lacked Axl, thus demonstrating that Axl possesses a similar epidermal expression distribution as observed for TGF-β1 (Bauer et al., 2012). Consistently, a portion of ex vivo isolated LCs lacked Axl (Bauer et al., 2012). The finding that only a portion of mouse LCs show activation of Smad2/3 proteins (Bobr et al., 2012) is in line with the model proposed here, that TGF-β1 is constitutively active only in a subset of LCs.

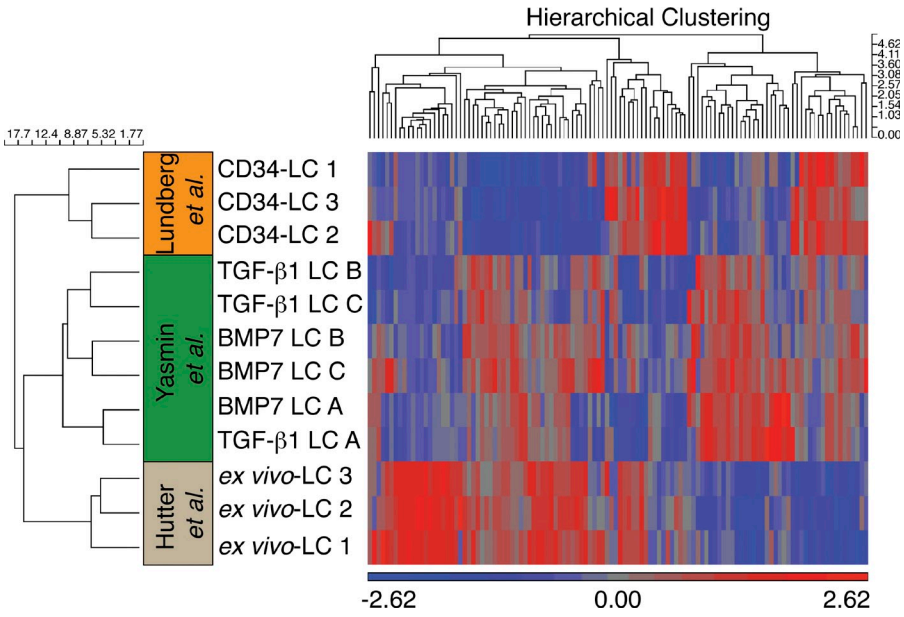


**Figure 7. Gene expression analysis.** Clustering using complete linkage algorithm on differentially expressed transcripts, identified by ANOVA analysis within multiple testing cutoff (false discovery rate is 5%, significance level is 0.05), demonstrates relationship among in vitro and ex vivo LCs. Heat map visualizing gene expression profiles of differentially expressed genes (listed in Table S1) upon hierarchical clustering with complete linkage and Euclidean measure. Colors represent high (red) and low (blue) normalized intensity. $CD1a^+CD207^+$ cells were generated from three independent donors (A, B, and C) in response to TGF-β1 or BMP7 and were flow sorted before analysis.

Four members of the BMP family can be detected in the epidermis (BMP2, BMP4, BMP6, and BMP7; Botchkarev, 2003). Among them, only BMP7 is expressed at high levels in basal keratinocyte layers. Moreover, we demonstrated here that BMP7 is strongly expressed in single-layered fetal epidermis at 8 wk EGA, a time point when LC precursors are first detectable in the epidermis. Our study is to our knowledge the first to show that BMP7 expression is detectable in basal/suprabasal epidermal layers during human prenatal development. In comparison, BMP6 is absent or only very weakly expressed in basal keratinocyte layers, and its expression correlates positively with increased keratinocyte differentiation (Lyons et al., 1989), similarly as shown for TGF-β1 (Bascom et al., 1989; Keski-Oja and Koli, 1992). It was previously noted that BMP7 and BMP6 exhibit opposite expression distribution among mouse epidermal keratinocyte layers (Lyons et al., 1989; Takahashi and Ikeda, 1996). The other BMPs, i.e., BMP2 and BMP4, are predominantly expressed in the hair follicle epithelium and mesenchyme, but not or only weakly in interfollicular epidermis (Lyons et al., 1989; Bitgood and McMahon, 1995).

Bmp7 KO mice exhibited substantially reduced numbers of LCs with the remaining LCs being morphologically less dendritic as compared with LCs from WT littermates. Therefore, we here described nonredundant positive effects of BMP7 on LC differentiation in vivo. However, our data do not rule out the possibility that other BMPs/type-1 receptor agonists may exert (partial) redundancy with BMP7 in promoting LC differentiation. The observations that epidermal transgenic expression of the BMP/activin inhibitor follistatin reduces LC numbers (Stoitzner et al., 2005) are consistent with a major role of the BMP–ALK3–Smad1/5/8 pathway in LC differentiation in vivo.

Our mechanistic insights into LC differentiation allowed us to design a greatly improved protocol for LC generation from $CD34^+$ HPCs in serum-free medium. Side-by-side analysis revealed that BMP7-supplemented cultures by far exceed TGF-β1–supplemented cultures in terms of absolute numbers of generated LCs as revealed by LC cluster formation and immunophenotypic analyses. Therefore, BMP7 signaling is sufficient to induce LCs. Additionally, BMP7 allowed the elimination of two other cytokines (i.e., SCF and TNF) from optimized LC generation cultures. Thus, a combination of only three cytokines, i.e., GM-CSF, FLT3L, and BMP7, with the late addition of TGF-β1 for 48 h, was found optimal for generating high yields of LCs. We showed that TGF-β1 induces LC generation via ALK3. However, the coactivation of ALK5 led to a reduction of LC generation. As a net effect, this led to only limited amounts of LC generation in previously optimized TGF-β1–dependent differentiation cultures of $CD34^+$ cells. A key finding of our study was that the replacement of TGF-β1 by BMP7 allows circumventing ALK5-mediated proliferation inhibition observed by TGF-β1. Consequently, BMP7 allows the generation of high numbers of LCs. Nevertheless, the late addition of TGF-β1 for the final 48 h was beneficial because it led to elevated percentages of generated LCs, potentially caused by a negative effect of TGF-β1 on cell proliferation. Additionally, late TGF-β1 led to inhibition of TLR-mediated proinflammatory cytokine production by LCs. In contrast, BMP7-generated LCs not exposed to TGF-β1 were highly potent inducers of T cell proliferation. This differential requirement might reflect in vivo niches and could help to explain differential T cell responses depending on the site of LC activation. In support of this concept, BMP7 LCs and TGF-β1 LCs differed in provoking Th1 versus Th2 responses in vitro. Moreover, this newly developed BMP7-dependent LC generation procedure with or without late TGF-β1 might be of interest for inducing strong antiviral/antitumor T cell responses. In conclusion, we here provide a mechanistic model for LC differentiation that utilizes two different family members of the TGF-β/BMP superfamily: BMP7 induces LC differentiation

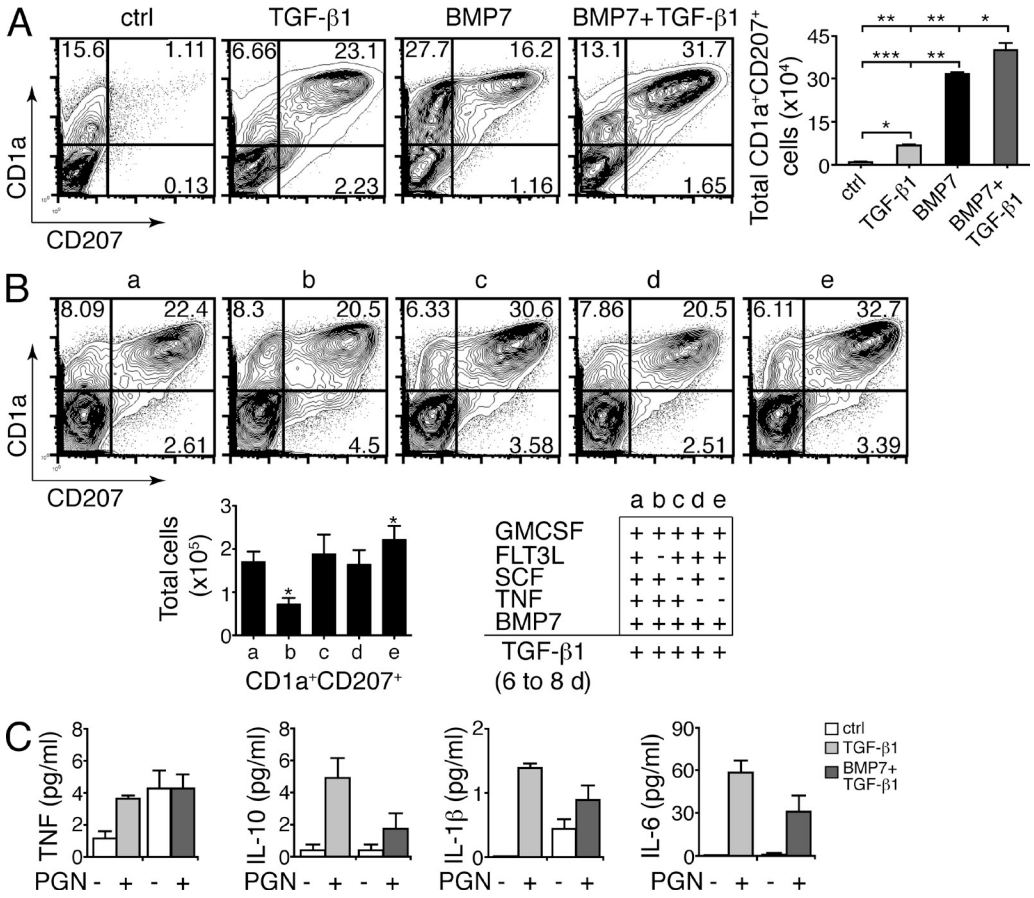


**Figure 8. Sequential addition of TGF-β1 to the BMP7-supplemented cultures enhances LC generation with minimal cytokine combination.** (A) CD34+ cells were induced to differentiate into LCs in response to TGF-β1 or BMP7 for 7 d. Parallel cultures contained BMP7 for 5 d, followed by TGF-β1 for the final 48 h (BMP7 + TGF-β1, right). Control cultures did not contain any exogenous TGF-β1 or BMP7 (left). All the cultures were supplemented with GM-CSF, TNF, SCF, and FLT3L. FACS plots represent day 7–generated cells analyzed for the expression of CD1a and CD207. Bar diagrams represent total numbers of CD1a+CD207+ cells observed in four independent experiments (±SD; *, $P < 0.05$; **, $P < 0.005$; ***, $P < 0.0005$). (B) LCs were generated in the presence of BMP7 for 6 d, followed by late TGF-β1 addition (48 h). In the first culture phase (days 1–6), different cytokine combinations were tested. FACS plots represent day 7–generated cells analyzed for the expression of CD1a and CD207. Bar diagrams represent mean total numbers of CD1a+CD207+ cells (±SEM) observed in three independent experiments. Graph represents different cytokine combinations used during LC differentiation as designated by a, b, c, d, and e (statistically significant: a vs. b, a vs. e, and b vs. e; *, $P < 0.05$). (C) LCs were generated in the presence of TGF-β1 for 7 d. Parallel cultures contained BMP7 for 5 d, followed by late addition of TGF-β1 (48 h; BMP7 + TGF-β1). All of the cultures were supplemented with GM-CSF, TNF, SCF, and FLT3L. LCs were cluster purified and activated or not with PGN for 48 h. Supernatants were collected for cytokine measurement. Bar diagrams represent mean amounts of cytokines produced in four independent experiments (mean ± SEM).

and proliferation, whereas TGF-β1 secures low levels of cytokine production by differentiated LCs, a potential prerequisite for postnatal LC network maintenance and function.

## MATERIALS AND METHODS

**Isolation of cells.** Cord blood samples were collected during healthy full-term deliveries. Approval was obtained from the Medical University of Vienna Institutional Review Board for these studies. Informed consent was provided in accordance with the Declaration of Helsinki. CD34+ cells were isolated as previously described (Taschner et al., 2007).

**Cytokines and reagents.** Human SCF, thrombopoietin (TPO), TNF, GM-CSF, FLT3L, IL-4, IL-6, BMP4, and BMP6 were purchased from PeproTech. TGF-β1 was purchased from R&D Systems. BMP7 and BMP2 were purchased from ImmunoTools. ALK4/5/7 inhibitor (SB431542) and ALK2/3/6 inhibitor (dorsomorphin dihydrochloride) were purchased from Tocris Bioscience.

**In vitro culture of CD34+ cord blood hematopoietic stem cells.** CD34+ cells were cultured for 2–3 d under progenitor expansion conditions (FLT3L, SCF, and TPO, each at 50 ng/ml) in serum-free medium (X-VIVO 15 medium; Bio Whittaker) before subculturing with lineage specific cytokines. LC cultures were described previously (Strobl et al., 1997). In brief, pre-expanded CD34+ cells (2–4 × $10^4$/ml per well) were cultured in 24-well tissue culture plates in serum-free CellGro DC medium (CellGenix) supplemented with 100 ng/ml GM-CSF, 20 ng/ml SCF, 50 ng/ml FLT3L, 2.5 ng/ml TNF, and 0.5 ng/ml TGF-β1 for 7 d. Cultures were supplemented with 2.5 mM GlutaMax (Gibco) and 125 U/ml each penicillin/streptomycin. LC clusters were purified as previously described (Gatti et al., 2000). For moDC generation, pre-expanded CD34+ cells (2–4 × $10^4$/ml per well) were first cultured in a 24-well plate in CellGro DC medium supplemented with 10% FCS in the presence of 100 ng/ml GM-CSF, 20 ng/ml SCF, 50 ng/ml FLT3L, and 2.5 ng/ml TNF for 4 d, followed by 100 ng/ml GM-CSF and 25 ng/ml IL-4 for 3 d in RPMI + 10% FCS medium (Jurkin et al., 2010).

For monocyte/macrophage generation, pre-expanded $CD34^+$ cells ($2–4 \times 10^4$/ml per well) were cultured in a 24-well plate in the presence of 100 ng/ml M-CSF, 20 ng/ml IL-6, 50 ng/ml FLT3L, and 100 ng/ml SCF in RPMI + 10% FCS medium (Heinz et al., 2006). When indicated, cell culture medium was supplemented with 200 ng/ml BMP7.

**RNA isolation and qRT-PCR.** RNA was isolated using the RNeasy Mini kit (QIAGEN). 1 µg RNA was reverse transcribed using Transcriptor First Strand cDNA kit (Roche) and oligo (dT) primers. Quantitative qRT-PCR analysis was performed as previously described (Yasmin et al., 2013). SYBR green and a CFX96 Real-Time PCR system (Bio-Rad Laboratories) were used for quantitative real-time PCR. Cycling conditions for qRT-PCR were 3 min at 95°C, followed by 40 cycles of 30 s at 95°C, 30 s at 60°C, and 30 s at 72°C. The following qRT-PCR primers were used: ALK2_F, 5′-TTGGAGACAGCACTTTAGCAG-3′; ALK2_R, 5′-GCGAGCCACTGTTCTTTGT-3′; ALK3_F, 5′-GAGTTGCTGCATTGCTGAC-3′; ALK3_R, 5′-GAGCCATGTAGCGTTTGGT-3′; ALK5_F, 5′-AGGCCAAATATCCCAAACAG-3′; ALK5_R, 5′-TAGCTGCTCCATTGGCATAC-3′; TGF-β1_F, 5′-GTACCTGAACCCGTGTTGCT-3′; TGF-β1_R, 5′-GTATCGCCAGGAATTGTTGC-3′; HPRT_F, 5′-GACCAGTCAACAGGGGACAT-3′; HPRT_R, 5′-AACACTTCGTGGGGTCCTTTTC-3′; TARC_F, 5′-CCATTCCCCTTAGAAAGCTG-3′; and TARC_R, 5′-CTCTCAAGGCTTTGCAGGTA-3′. Results were analyzed using the Δ ΔCt method and presented as fold difference in mRNA level relative to HPRT.

**Retroviral vectors, transfection of packaging cell lines, and gene transduction.** ALK2-HASLwt-IRES-GFP, ALK3-HASLwt-IRES-GFP, and ALK5-HASLwt-IRES-GFP were obtained by cutting ALK2-HASLwt-pCDNA3, ALK3-HASLwt-pCDNA3, and ALK5-HASLwt-pCDNA3 (gift of P. ten Dijke, Leiden University Medical Center, Leiden Netherlands) with EcoRI and XhoI and inserting it into the PBMN-IRES-GFP vector. Transfection of packaging cell line phoenix-GP as well as infection of target cells was performed as previously described (Platzer et al., 2004). In brief, to produce recombinant amphotropic retrovirus, vectors were transiently transfected into the packaging cell line Phoenix-GP (Gag-Pol) using a calcium-phosphate protocol (Platzer et al., 2004). Phoenix-GP was cotransfected with an expression plasmid encoding gibbon ape leukemia virus (GALV) envelope (gift from D.B. Kohn, University of California, Los Angeles, Los Angeles, CA). Before gene transduction, fresh or thawed $CD34^+$ cells were stimulated overnight in X-VIVO 15 medium supplemented with the cytokines SCF (50 ng/ml), FLT3L (50 ng/ml), and TPO (50 ng/ml). Afterward, 1 ml of retroviral supernatant (harvested 36–48 h after transfection of packaging cells) was added to $4 \times 10^4$ $CD34^+$ HPCs in the presence of plate-bound RetroNectin (Takara Bio Inc.) using nontissue culture–treated 24-well plates (Cellstar; Greiner Bio-One GmbH) according to the instructions of the manufacturer. Infections were repeated two to three times at intervals of 12–24 h using fresh virus supernatants in the presence of cytokines SCF, FLT3L, and TPO. Within 60 h of the first transduction cycle, cells were harvested and recultured in LC, moDC, and monocyte/macrophage lineage conditions.

**Immunofluorescence and immunohistochemistry.** Prenatal and adult skin specimens were embedded in optimum cutting tissue compound (Tissue-Tek; Sakura), snap frozen in liquid nitrogen, and stored at −80°C until further processing. 6-µm sections were cut, air dried, fixed in ice-cold acetone for 10 min, blocked with PBS 2% BSA for 1 h at room temperature, and stained with the primary unconjugated control rabbit isotype IgG (1:200; Santa Cruz Biotechnology, Inc.) or antibodies specific for BMP4 (1:100; Abcam) or BMP7 (1:200; LifeSpan Biosciences) overnight at 4°C. The slides were washed with PBS and stained with the secondary goat anti–rabbit Alexa Fluor 546 (Invitrogen) for 2 h at room temperature. Alexa Fluor 488 anti-Laminin5 (EMD Millipore) was used to visualize the dermo-epidermal junction. Nuclei were stained with DAPI. Pictures were taken using an LSM700 microscope and Zen 2009 software (Carl Zeiss). For immunohistochemistry, human tissue sections were then incubated with anti-LAP (R&D Systems) and anti–TGF-β1 serum (Santa Cruz Biotechnology, Inc.) overnight at 4°C, followed by biotin-conjugated goat anti–rabbit IgG for 2 h at room temperature using the Elite rabbit IgG VECTASTAIN kits. Biotinylated antibodies were detected with HRP streptavidin and staining was visualized with amino-ethylcarbazole (AEC; Dako). Finally, sections were mounted with Aquatex (Merck) and examined using an Eclipse 80 microscope (Nikon). Mouse epidermal sheets were prepared as described previously (Bauer et al., 2012). Epidermis was fixed in acetone for 10–20 min, blocked with PBS containing 2% BSA for 1 h at room temperature, and stained with antibody specific for I-A/I-E (PE-conjugated; 1:400; BioLegend) overnight at 4°C. The slides were washed with PBS and stained with DAPI to visualize the nuclei. Images from seven randomly chosen microscopic fields were acquired. LCs were enumerated, and mean values were calculated per ear sheet. Pictures were taken using an Eclipse 80i microscope (Nikon) and Lucia G software (Laboratory Imaging).

**RNA isolation, amplification, and gene chip hybridization.** Total RNA from three independent donors was isolated from sorted cells by using the RNeasy Micro kit (QIAGEN) according to the manufacturer's recommendations. Quality control with the RNA 6000 Pico LabChip kit (Agilent Technologies) on a BioAnalyzer 2100 (Agilent Technologies) showed a RIN of 9.9–10. cRNA target synthesis, amplification, hybridization to the GeneChip Human Genome U133 Plus 2.0 array, and scanning were performed according to the standard protocols recommended by the manufacturer (Affymetrix). In brief, cDNA was generated from 50 ng of total RNA using T7–oligo (dT) promoter primer (GeneChip 3′ IVT Express kit; Affymetrix). After a second strand cDNA synthesis, cDNA was converted to cRNA by an in vitro transcription reaction (Life Technologies). Thereafter, cRNA was purified, and the yield was controlled with a spectrophotometer. Labeled cRNA was purified, quality controlled with the BioAnalyzer 2100, and denatured at 94°C before hybridization of 12 µg of the purified sample. The samples were hybridized to the Human Genome U133 Plus 2.0 Array at 45°C for 16 h (60 rpm) in an hybridization oven. The arrays were then processed on the GeneChip fluidics station 450: protocol FS450_0001 for Cartridge Arrays. They were washed, stained with streptavidin-PE (GeneChip HT hybridization Wash and Stain kit; Affymetrix), washed again, and scanned with a GeneArray scanner (GCS3000; Affymetrix).

Raw and normalized microarray experiments have been submitted to the GEO database (accession no. GSE49085). Fluorescent intensity was analyzed using the GeneChip Operating Software (GCOS) 1.1 (Affymetrix) and scaled to a target value of 100. Data uploaded into Expression Console EC1.2.1.20 (Affymetrix), normalized with the MAS5 algorithm and for log transformed data (Robust Multi-Array [RMA]), were used for the generation of CEL-files. The intensities <200 were considered to be below positive expression and compared with signal intensities of previously published arrays (Lundberg et al., 2013; MAS5 normalized data; Table S1). Transcripts differentially expressed among all samples were identified using ANOVA analysis within multiple testing cutoff (false discovery rate is 5%, significance level is 0.05). Relationship between different cell populations was demonstrated by the minimal spanning tree analysis. Additionally, hierarchical clustering was performed using Cluster 3.0, based on complete linkage and Euclidean distance measure, and heat maps of selected genes (listed in Table S1) were subsequently produced using Java Treeview 1.0.12. Fold change of transcripts ≥ 1.5 was considered as up-regulation and vice versa. Fold change of important transcripts was compared with different subsets of LCs as described in Table S2.

***Bmp7*$^{\Delta/\Delta}$ mice and LacZ staining of tissues.** The generation of *Bmp7*$^{\Delta/\Delta}$ mice has previously been described (Zouvelou et al., 2009). All mouse lines were backcrossed for more than eight generations into the C57BL/6J background. Tissues from heterozygous *Bmp7lacZ* (*Bmp7*$^{wt/lacZ}$) mice (expressing β-galactosidase under the control of the *Bmp7* promoter) were stained with X-gal to identify the location of *Bmp7* expression. In brief, isolated epidermal tissue was fixed in 2% formaldehyde, 0.2% glutaraldehyde, 0.01% sodium deoxycholate, 0.02% NP-40 in PBS for 5 min, washed with 2 mM $MgCl_2$, and stained at room temperature in the dark for several hours to overnight in X-gal staining solution, which contained 0.1 M phosphate, pH 7.3, 2 mM $MgCl_2$, 0.01% sodium deoxycholate, 0.02% NP-40, 5 mM $K_3[Fe(CN)_6]$, and

5 mM $K_4[Fe(CN)_6]$ supplemented with 1 mg X-Gal (Promega)/ml. The samples were washed and refixed in 4% PFA and mounted with water-based Mowiol 4-88 (Sigma-Aldrich) and documented using a DM-E microscope equipped with a DFC290 camera (Leica). Experimental results were obtained from at least three independent samples. Mice were maintained at the animal facilities of the University of Zurich. Animal experiments were approved by the local veterinary authorities (permit 98/2011, Veterinäramt Zürich) in compliance with Swiss federal law (TSchG, TSchV) and cantonal by-laws in full compliance with the European Guideline 86/609/EC. This authority approval also included ethical approval.

**Western blot analysis.** Cells were directly lysed in 1× SDS-loading dye at 95°C for 5 min. For Western blot analysis, lysates of 1–2 × $10^5$ cells per lane were loaded on 10% SDS-polyacrylamide gels. Resolved proteins were transferred to a polyvinylidene-difluoride membrane (Immobilon-P; EMD Millipore) as previously described (Yasmin et al., 2013). Membranes were probed with antibodies against rabbit-pSmad1 (Ser463/465)/Smad5 (Ser463/465)/Smad8 (Ser426/428), rabbit-pSmad2 (Ser465/467), and rabbit-pSmad3 (Ser423/425; Cell Signaling Technology), rabbit-Smad1/5/8 (N-18)-R, and goat-Smad2/3 (E-20; Santa Cruz Biotechnology, Inc.), followed by HRP-conjugated goat anti–rabbit, rabbit anti–goat (Thermo Fisher Scientific). Detection was performed with the chemiluminescent substrate SuperSignal WestPico or WestDura (Thermo Fisher Scientific).

**Flow cytometry.** Flow cytometry staining and analysis were performed as described previously (Yasmin et al., 2013). Mouse mAbs of the following specificities were used: FITC-conjugated mAb specific for CD1a, PE-conjugated mAb specific for CD207 (Immunotech), allophycocyanin-conjugated antibody for CD324, Pacific blue–conjugated CD1a and CD14 (APC-CY7; BioLegend), CD11b (PE-CY7; BD), and MPO-C2 (PE; AN DER GRUB Bio Research GmbH). All stainings were performed with permeabilized cells. Flow cytometric analysis was performed using an LSRII instrument (BD) and FlowJo software (Tree Star).

**T cell proliferation assays.** T cell proliferation assay (MLR) was performed as described previously (Stöckl et al., 1999). In brief, purified LC clusters were seeded (5 × $10^4$ to $10^5$/500 µl) in a 48-well plate and activated with PGN. Graded numbers of these stimulator cells were co-cultured with a constant number of 5 × $10^4$ to $10^5$ highly purified (>98%) allogeneic T cells in RPMI medium containing 10% FCS using round-bottom, 96-well tissue culture plates (Nalge Europe). Proliferation of T cells was monitored on day 5 of culture by adding [methyl-$^3$H]TdR followed by measuring [methyl-$^3$H]TdR incorporation 18 h later. Incorporated radioactivity was measured using a 1450 microbeta plate reader (Wallac-Trilux Instrument; Life Science). The basal proliferation rate of T cell control was 900 ± 200 cell counts. Supernatants were collected for cytokine measurement before adding [methyl-$^3$H]TdR. Assays were performed in triplicates.

**Cytokine measurement.** Purified LC clusters were seeded (5 × $10^4$ to $10^5$/500 µl) in a 48-well plate. Cells were activated with PGN, and supernatants were collected 48 h later as described previously (Jurkin et al., 2010). Quantification of cytokines produced by LCs or LC/T cell co-cultures was performed using the Luminex system (Austin, TX).

**Statistical analysis.** Statistical analysis was performed using the paired, two-tailed Student's *t* test or ANOVA; p-values of <0.05 were considered significant.

**Online supplemental material.** Table S1 shows comparison of expression levels of important transcripts in LCs. Table S2 shows comparison of fold change of important transcripts in LCs. Online supplemental material is available at http://www.jem.org/cgi/content/full/jem.20130275/DC1.

G. Zlabinger, M. Merio, and P. Waidhofer-Söllner are acknowledged for performing cytokine measurements.

This work was supported by a PhD fellowship of the High Education Commission of Pakistan to N. Yasmin, Austrian Science Fund (FWF) grants P22058, P19245, P25720, and SFB-2304 to H. Strobl and P23215-B11 to R. Köffel, PhD program W1212 "Inflammation and Immunity" to T. Bauer, and FWF grant P19474-B13 to A. Elbe-Bürger.

The authors have no financial conflicts of interest.

**Submitted: 7 February 2013**
**Accepted: 7 October 2013**

## REFERENCES

Bascom, C.C., J.R. Wolfshohl, R.J. Coffey Jr., L. Madisen, N.R. Webb, A.R. Purchio, R. Derynck, and H.L. Moses. 1989. Complex regulation of transforming growth factor beta 1, beta 2, and beta 3 mRNA expression in mouse fibroblasts and keratinocytes by transforming growth factors beta 1 and beta 2. *Mol. Cell. Biol.* 9:5508–5515.

Bauer, T., A. Zagórska, J. Jurkin, N. Yasmin, R. Köffel, S. Richter, B. Gesslbauer, G. Lemke, and H. Strobl. 2012. Identification of Axl as a downstream effector of TGF-β1 during Langerhans cell differentiation and epidermal homeostasis. *J. Exp. Med.* 209:2033–2047. http://dx.doi.org/10.1084/jem.20120493

Bitgood, M.J., and A.P. McMahon. 1995. Hedgehog and Bmp genes are coexpressed at many diverse sites of cell-cell interaction in the mouse embryo. *Dev. Biol.* 172:126–138. http://dx.doi.org/10.1006/dbio.1995.0010

Bobr, A., B.Z. Igyarto, K.M. Haley, M.O. Li, R.A. Flavell, and D.H. Kaplan. 2012. Autocrine/paracrine TGF-β1 inhibits Langerhans cell migration. *Proc. Natl. Acad. Sci. USA.* 109:10492–10497. http://dx.doi.org/10.1073/pnas.1119178109

Borkowski, T.A., J.J. Letterio, A.G. Farr, and M.C. Udey. 1996. A role for endogenous transforming growth factor β1 in Langerhans cell biology: the skin of transforming growth factor β1 null mice is devoid of epidermal Langerhans cells. *J. Exp. Med.* 184:2417–2422. http://dx.doi.org/10.1084/jem.184.6.2417

Botchkarev, V.A. 2003. Bone morphogenetic proteins and their antagonists in skin and hair follicle biology. *J. Invest. Dermatol.* 120:36–47. http://dx.doi.org/10.1046/j.1523-1747.2003.12002.x

Botchkarev, V.A., N.V. Botchkareva, W. Roth, M. Nakamura, L.H. Chen, W. Herzog, G. Lindner, J.A. McMahon, C. Peters, R. Lauster, et al. 1999. Noggin is a mesenchymally derived stimulator of hair-follicle induction. *Nat. Cell Biol.* 1:158–164. http://dx.doi.org/10.1038/11078

Caux, C., C. Dezutter-Dambuyant, D. Schmitt, and J. Banchereau. 1992. GM-CSF and TNF-alpha cooperate in the generation of dendritic Langerhans cells. *Nature.* 360:258–261. http://dx.doi.org/10.1038/360258a0

Caux, C., C. Massacrier, B. Dubois, J. Valladeau, C. Dezutter-Dambuyant, I. Durand, D. Schmitt, and S. Saeland. 1999. Respective involvement of TGF-beta and IL-4 in the development of Langerhans cells and non-Langerhans dendritic cells from CD34+ progenitors. *J. Leukoc. Biol.* 66:781–791.

Chang-Rodriguez, S., W. Hoetzenecker, C. Schwärzler, T. Biedermann, S. Saeland, and A. Elbe-Bürger. 2005. Fetal and neonatal murine skin harbors Langerhans cell precursors. *J. Leukoc. Biol.* 77:352–360. http://dx.doi.org/10.1189/jlb.1004584

Chorro, L., A. Sarde, M. Li, K.J. Woollard, P. Chambon, B. Malissen, A. Kissenpfennig, J.B. Barbaroux, R. Groves, and F. Geissmann. 2009. Langerhans cell (LC) proliferation mediates neonatal development, homeostasis, and inflammation-associated expansion of the epidermal LC network. *J. Exp. Med.* 206:3089–3100. http://dx.doi.org/10.1084/jem.20091586

Daly, A.C., R.A. Randall, and C.S. Hill. 2008. Transforming growth factor beta-induced Smad1/5 phosphorylation in epithelial cells is mediated by novel receptor complexes and is essential for anchorage-independent growth. *Mol. Cell. Biol.* 28:6889–6902. http://dx.doi.org/10.1128/MCB.01192-08

Dennler, S., M.J. Goumans, and P. ten Dijke. 2002. Transforming growth factor beta signal transduction. *J. Leukoc. Biol.* 71:731–740.

Ebner, R., R.H. Chen, S. Lawler, T. Zioncheck, and R. Derynck. 1993. Determination of type I receptor specificity by the type II receptors for TGF-beta or activin. *Science.* 262:900–902. http://dx.doi.org/10.1126/science.8235612

Elbe, A., E. Tschachler, G. Steiner, A. Binder, K. Wolff, and G. Stingl. 1989. Maturational steps of bone marrow-derived dendritic murine epidermal cells. Phenotypic and functional studies on Langerhans cells and Thy-1+ dendritic epidermal cells in the perinatal period. *J. Immunol.* 143:2431–2438.

Fainaru, O., E. Woolf, J. Lotem, M. Yarmus, O. Brenner, D. Goldenberg, V. Negreanu, Y. Bernstein, D. Levanon, S. Jung, and Y. Groner. 2004. Runx3 regulates mouse TGF-beta-mediated dendritic cell function and its absence results in airway inflammation. *EMBO J.* 23:969–979. http://dx.doi.org/10.1038/sj.emboj.7600085

Feng, X.H., and R. Derynck. 2005. Specificity and versatility in tgf-beta signaling through Smads. *Annu. Rev. Cell Dev. Biol.* 21:659–693. http://dx.doi.org/10.1146/annurev.cellbio.21.022404.142018

Gatti, E., M.A. Velleca, B.C. Biedermann, W. Ma, J. Unternaehrer, M.W. Ebersold, R. Medzhitov, J.S. Pober, and I. Mellman. 2000. Large-scale culture and selective maturation of human Langerhans cells from granulocyte colony-stimulating factor-mobilized CD34+ progenitors. *J. Immunol.* 164:3600–3607.

Geissmann, F., C. Prost, J.P. Monnet, M. Dy, N. Brousse, and O. Hermine. 1998. Transforming growth factor β1, in the presence of granulocyte/macrophage colony-stimulating factor and interleukin 4, induces differentiation of human peripheral blood monocytes into dendritic Langerhans cells. *J. Exp. Med.* 187:961–966. http://dx.doi.org/10.1084/jem.187.6.961

Geissmann, F., P. Revy, A. Regnault, Y. Lepelletier, M. Dy, N. Brousse, S. Amigorena, O. Hermine, and A. Durandy. 1999. TGF-beta 1 prevents the noncognate maturation of human dendritic Langerhans cells. *J. Immunol.* 162:4567–4575.

Goumans, M.J., G. Valdimarsdottir, S. Itoh, A. Rosendahl, P. Sideras, and P. ten Dijke. 2002. Balancing the activation state of the endothelium via two distinct TGF-beta type I receptors. *EMBO J.* 21:1743–1753. http://dx.doi.org/10.1093/emboj/21.7.1743

Gupta, A.K., C. Rusterholz, W. Holzgreve, and S. Hahn. 2005. Constant IFNgamma mRNA to protein ratios in cord and adult blood T cells suggests regulation of IFNgamma expression in cord blood T cells occurs at the transcriptional level. *Clin. Exp. Immunol.* 140:282–288. http://dx.doi.org/10.1111/j.1365-2249.2005.02758.x

Hacker, C., R.D. Kirsch, X.S. Ju, T. Hieronymus, T.C. Gust, C. Kuhl, T. Jorgas, S.M. Kurz, S. Rose-John, Y. Yokota, and M. Zenke. 2003. Transcriptional profiling identifies Id2 function in dendritic cell development. *Nat. Immunol.* 4:380–386. http://dx.doi.org/10.1038/ni903

Heinz, L.X., B. Platzer, P.M. Reisner, A. Jörgl, S. Taschner, F. Göbel, and H. Strobl. 2006. Differential involvement of PU.1 and Id2 downstream of TGF-beta1 during Langerhans-cell commitment. *Blood.* 107:1445–1453. http://dx.doi.org/10.1182/blood-2005-04-1721

Helder, M.N., E. Ozkaynak, K.T. Sampath, F.P. Luyten, V. Latin, H. Oppermann, and S. Vukicevic. 1995. Expression pattern of osteogenic protein-1 (bone morphogenetic protein-7) in human and mouse development. *J. Histochem. Cytochem.* 43:1035–1044. http://dx.doi.org/10.1177/43.10.7560881

Hoshino, N., N. Katayama, T. Shibasaki, K. Ohishi, J. Nishioka, M. Masuya, Y. Miyahara, M. Hayashida, D. Shimomura, T. Kato, et al. 2005. A novel role for Notch ligand Delta-1 as a regulator of human Langerhans cell development from blood monocytes. *J. Leukoc. Biol.* 78:921–929. http://dx.doi.org/10.1189/jlb.1204746

Hutter, C., M. Kauer, I. Simonitsch-Klupp, G. Jug, R. Schwentner, J. Leitner, P. Bock, P. Steinberger, W. Bauer, N. Carlesso, et al. 2012. Notch is active in Langerhans cell histiocytosis and confers pathognomonic features on dendritic cells. *Blood.* 120:5199–5208. http://dx.doi.org/10.1182/blood-2012-02-410241

Hwang, E.A., H.B. Lee, and K.C. Tark. 2001. Comparison of bone morphogenetic protein receptors expression in the fetal and adult skin. *Yonsei Med. J.* 42:581–586.

Igyártó, B.Z., and D.H. Kaplan. 2013. Antigen presentation by Langerhans cells. *Curr. Opin. Immunol.* 25:115–119. http://dx.doi.org/10.1016/j.coi.2012.11.007

Izumi, N., S. Mizuguchi, Y. Inagaki, S. Saika, N. Kawada, Y. Nakajima, K. Inoue, S. Suehiro, S.L. Friedman, and K. Ikeda. 2006. BMP-7 opposes TGF-beta1-mediated collagen induction in mouse pulmonary myofibroblasts through Id2. *Am. J. Physiol. Lung Cell. Mol. Physiol.* 290:L120–L126. http://dx.doi.org/10.1152/ajplung.00171.2005

Jurkin, J., Y.M. Schichl, R. Koeffel, T. Bauer, S. Richter, S. Konradi, B. Gesslbauer, and H. Strobl. 2010. miR-146a is differentially expressed by myeloid dendritic cell subsets and desensitizes cells to TLR2-dependent activation. *J. Immunol.* 184:4955–4965. http://dx.doi.org/10.4049/jimmunol.0903021

Kane, C.J., A.M. Knapp, J.N. Mansbridge, and P.C. Hanawalt. 1990. Transforming growth factor-beta 1 localization in normal and psoriatic epidermal keratinocytes in situ. *J. Cell. Physiol.* 144:144–150. http://dx.doi.org/10.1002/jcp.1041440119

Kaplan, D.H., M.O. Li, M.C. Jenison, W.D. Shlomchik, R.A. Flavell, and M.J. Shlomchik. 2007. Autocrine/paracrine TGFβ1 is required for the development of epidermal Langerhans cells. *J. Exp. Med.* 204:2545–2552. http://dx.doi.org/10.1084/jem.20071401

Kel, J.M., M.J. Girard-Madoux, B. Reizis, and B.E. Clausen. 2010. TGF-beta is required to maintain the pool of immature Langerhans cells in the epidermis. *J. Immunol.* 185:3248–3255. http://dx.doi.org/10.4049/jimmunol.1000981

Keski-Oja, J., and K. Koli. 1992. Enhanced production of plasminogen activator activity in human and murine keratinocytes by transforming growth factor-beta 1. *J. Invest. Dermatol.* 99:193–200. http://dx.doi.org/10.1111/1523-1747.ep12616826

Krystal, G., V. Lam, W. Dragowska, C. Takahashi, J. Appel, A. Gontier, A. Jenkins, H. Lam, L. Quon, and P. Lansdorp. 1994. Transforming growth factor beta 1 is an inducer of erythroid differentiation. *J. Exp. Med.* 180:851–860. http://dx.doi.org/10.1084/jem.180.3.851

Li, A.G., S.L. Lu, G. Han, K.E. Hoot, and X.J. Wang. 2006. Role of TGFbeta in skin inflammation and carcinogenesis. *Mol. Carcinog.* 45:389–396. http://dx.doi.org/10.1002/mc.20229

Lundberg, K., A.S. Albrekt, I. Nelissen, S. Santegoets, T.D. de Gruijl, S. Gibbs, and M. Lindstedt. 2013. Transcriptional profiling of human dendritic cell populations and models—unique profiles of in vitro dendritic cells and implications on functionality and applicability. *PLoS ONE.* 8:e52875. http://dx.doi.org/10.1371/journal.pone.0052875

Lyons, K.M., R.W. Pelton, and B.L. Hogan. 1989. Patterns of expression of murine Vgr-1 and BMP-2a RNA suggest that transforming growth factor-beta-like genes coordinately regulate aspects of embryonic development. *Genes Dev.* 3:1657–1668. http://dx.doi.org/10.1101/gad.3.11.1657

Massagué, J. 1998. TGF-beta signal transduction. *Annu. Rev. Biochem.* 67:753–791. http://dx.doi.org/10.1146/annurev.biochem.67.1.753

Merad, M., M.G. Manz, H. Karsunky, A. Wagers, W. Peters, I. Charo, I.L. Weissman, J.G. Cyster, and E.G. Engleman. 2002. Langerhans cells renew in the skin throughout life under steady-state conditions. *Nat. Immunol.* 3:1135–1141. http://dx.doi.org/10.1038/ni852

Miyazono, K., Y. Kamiya, and M. Morikawa. 2010. Bone morphogenetic protein receptors and signal transduction. *J. Biochem.* 147:35–51. http://dx.doi.org/10.1093/jb/mvp148

Oh, S.P., T. Seki, K.A. Goss, T. Imamura, Y. Yi, P.K. Donahoe, L. Li, K. Miyazono, P. ten Dijke, S. Kim, and E. Li. 2000. Activin receptor-like kinase 1 modulates transforming growth factor-beta 1 signaling in the regulation of angiogenesis. *Proc. Natl. Acad. Sci. USA.* 97:2626–2631. http://dx.doi.org/10.1073/pnas.97.6.2626

Platzer, B., A. Jörgl, S. Taschner, B. Höcher, and H. Strobl. 2004. RelB regulates human dendritic cell subset development by promoting monocyte intermediates. *Blood.* 104:3655–3663. http://dx.doi.org/10.1182/blood-2004-02-0412

Romani, N., G. Schuler, and P. Fritsch. 1986. Ontogeny of Ia-positive and Thy-1-positive leukocytes of murine epidermis. *J. Invest. Dermatol.* 86:129–133. http://dx.doi.org/10.1111/1523-1747.ep12284135

Romani, N., P.M. Brunner, and G. Stingl. 2012. Changing views of the role of Langerhans cells. *J. Invest. Dermatol.* 132:872–881. http://dx.doi.org/10.1038/jid.2011.437

Schmierer, B., and C.S. Hill. 2007. TGFbeta-SMAD signal transduction: molecular specificity and functional flexibility. *Nat. Rev. Mol. Cell Biol.* 8:970–982. http://dx.doi.org/10.1038/nrm2297

Schuster, C., C. Vaculik, C. Fiala, S. Meindl, O. Brandt, M. Imhof, G. Stingl, W. Eppel, and A. Elbe-Bürger. 2009. HLA-DR$^+$ leukocytes

acquire CD1 antigens in embryonic and fetal human skin and contain functional antigen-presenting cells. *J. Exp. Med.* 206:169–181. http://dx.doi.org/10.1084/jem.20081747

Stöckl, J., H. Vetr, O. Majdic, G. Zlabinger, E. Kuechler, and W. Knapp. 1999. Human major group rhinoviruses downmodulate the accessory function of monocytes by inducing IL-10. *J. Clin. Invest.* 104:957–965. http://dx.doi.org/10.1172/JCI7255

Stoitzner, P., H. Stössel, M. Wankell, S. Hofer, C. Heufler, S. Werner, and N. Romani. 2005. Langerhans cells are strongly reduced in the skin of transgenic mice overexpressing follistatin in the epidermis. *Eur. J. Cell Biol.* 84:733–741. http://dx.doi.org/10.1016/j.ejcb.2005.04.003

Strobl, H., E. Riedl, C. Scheinecker, C. Bello-Fernandez, W.F. Pickl, K. Rappersberger, O. Majdic, and W. Knapp. 1996. TGF-beta 1 promotes in vitro development of dendritic cells from CD34+ hemopoietic progenitors. *J. Immunol.* 157:1499–1507.

Strobl, H., C. Bello-Fernandez, E. Riedl, W.F. Pickl, O. Majdic, S.D. Lyman, and W. Knapp. 1997. flt3 ligand in cooperation with transforming growth factor-beta1 potentiates in vitro development of Langerhans-type dendritic cells and allows single-cell dendritic cell cluster formation under serum-free conditions. *Blood.* 90:1425–1434.

Takahashi, H., and T. Ikeda. 1996. Transcripts for two members of the transforming growth factor-beta superfamily BMP-3 and BMP-7 are expressed in developing rat embryos. *Dev. Dyn.* 207:439–449. http://dx.doi.org/10.1002/(SICI)1097-0177(199612)207:4<439::AID-AJA8>3.0.CO;2-I

Taschner, S., C. Koesters, B. Platzer, A. Jörgl, W. Ellmeier, T. Benesch, and H. Strobl. 2007. Down-regulation of RXRalpha expression is essential for neutrophil development from granulocyte/monocyte progenitors. *Blood.* 109:971–979. http://dx.doi.org/10.1182/blood-2006-04-020552

Xu, Y.P., Y. Shi, Z.-Z. Cui, H.H. Jiang, L. Li, X.-F. Wang, L. Zhou, and Q.-S. Mi. 2012. TGFβ/Smad3 signal pathway is not required for epidermal Langerhans cell development. *J. Invest. Dermatol.* 132:2106–2109. http://dx.doi.org/10.1038/jid.2012.71

Yasmin, N., S. Konradi, G. Eisenwort, Y.M. Schichl, M. Seyerl, T. Bauer, J. Stöckl, and H. Strobl. 2013. β-Catenin promotes the differentiation of epidermal Langerhans dendritic cells. *J. Invest. Dermatol.* 133:1250–1259. http://dx.doi.org/10.1038/jid.2012.481

Young, J.W., P. Szabolcs, and M.A. Moore. 1995. Identification of dendritic cell colony-forming units among normal human CD34+ bone marrow progenitors that are expanded by c-kit-ligand and yield pure dendritic cell colonies in the presence of granulocyte/macrophage colony-stimulating factor and tumor necrosis factor alpha. *J. Exp. Med.* 182:1111–1119. http://dx.doi.org/10.1084/jem.182.4.1111

Zahner, S.P., J.M. Kel, C.A. Martina, I. Brouwers-Haspels, M.A. van Roon, and B.E. Clausen. 2011. Conditional deletion of TGF-βR1 using Langerin-Cre mice results in Langerhans cell deficiency and reduced contact hypersensitivity. *J. Immunol.* 187:5069–5076. http://dx.doi.org/10.4049/jimmunol.1101880

Zouvelou, V., O. Passa, K. Segklia, S. Tsalavos, D.M. Valenzuela, A.N. Economides, and D. Graf. 2009. Generation and functional characterization of mice with a conditional BMP7 allele. *Int. J. Dev. Biol.* 53:597–603. http://dx.doi.org/10.1387/ijdb.082648vz